# A SIRV-CFAR Adaptive Detector Exploiting Persymmetric Clutter Covariance Structure

Guilhem Pailloux[12], Jean-Philippe Ovarlez[1], Frédéric Pascal[3] and Philippe Forster[2]

[1] ONERA - DEMR/TSI, Chemin de la Hunière, F-91120 Palaiseau, France
[2] GEA, 1 Chemin Desvallières, F-92410 Ville d'Avray, France
[3] SATIE, ENS Cachan, CNRS, UniverSud, 61 Av. du Pdt Wilson, F-94235 Cachan, France

e-mail: guilhem.pailloux@onera.fr, jean-philippe.ovarlez@onera.fr,
frederic.pascal@satie.ens-cachan.fr, philippe.forster@u-paris10.fr

***Abstract*—This paper deals with covariance matrix estimation for radar detection in non-Gaussian noise modeled by Spherically Invariant Random Vector (SIRV). In many applications, it is possible to assume a particular structure for the clutter covariance matrix: this is the case for instance for active systems using a symmetrically spaced linear array or pulse train. In this paper, we propose to use the particular persymmetric structure of the matrix to improve performance in term of detection.**
**In this context, we provide a new adaptive detector and derive its statistical properties as well as its statistical distribution. Moreover, the high improvement of its detection performance is demonstrated on experimental ground clutter data.**

***Index Terms*—Radar detection, Non-Gaussian clutter, SIRV**

## I. Introduction

One of the main problems in radar consists in detecting a target embedded in clutter returns using a coherent pulse train. In recent years, there has been an increasing interest for non-Gaussian clutter models motivated by experimental radar clutter measurements [1]. Based on this experimental evidence, it has been shown that clutter returns are accurately modeled as Spherically Invariant Random Vector (SIRV) consisting in the product of a Gaussian vector - called speckle - with the square root of a positive random variable - called texture [2], [3]. In this context, the basic problem of detecting a known signal $\mathbf{p} \in \mathbb{C}^m$ corrupted by an additive SIRV clutter $\mathbf{c}$ can be stated as the following binary hypothesis test:

$$\begin{cases} H_0 : \mathbf{y} = \mathbf{c}, & \mathbf{y}_k = \mathbf{c}_k, \ \text{for } 1 \leq k \leq K\,, \\ H_1 : \mathbf{y} = A\,\mathbf{p} + \mathbf{c}, & \mathbf{y}_k = \mathbf{c}_k, \ \text{for } 1 \leq k \leq K\,, \end{cases} \tag{1}$$

where $\mathbf{y}$ is the complex $m$-vector of the received signal, $A$ is an unknown complex target amplitude, $\mathbf{p}$ stands for the known "steering vector" and $\mathbf{c}$ is a SIRV noise. More precisely, $\mathbf{c}$ is the product of the square root of a positive random variable $\tau$ (texture) and a $m$-dimensional independent complex Gaussian vector $\mathbf{g}$ (speckle) with zero-mean and covariance matrix $\mathbf{M}$ normalized according to $\text{Tr}(\mathbf{M}) = m$:

$$\mathbf{c} = \sqrt{\tau}\,\mathbf{g}\,. \tag{2}$$

Under both hypotheses, it is assumed that $K$ signal-free data $\mathbf{y}_k$ are available for clutter parameters estimation. The $\mathbf{y}_k$'s are the so-called secondary data. They are independent and identically distributed (i.i.d) with the same distribution as $\mathbf{c}$.

In the sequel, the real (resp. complex) Gaussian distribution with zero-mean and covariance matrix $\mathbf{M}$ is denoted by $\mathcal{N}(\mathbf{0}, \mathbf{M})$ (resp. $\mathcal{CN}(\mathbf{0}, \mathbf{M})$), $E[.]$ stands for the expectation operator, $^H$ denotes the transpose conjugate, $^*$ the conjugate and $^\top$ the transpose operator, $\|\,.\,\|$ is the usual $\mathcal{L}^2$-norm, $\mathbf{I}_m$ is the *m*-th order identity matrix and $\sim$ means "distributed as".

When $\mathbf{M}$ is known, this model has been widely studied and allows to build a Generalized Likelihood Ratio Test - Linear Quadratic (GLRT-LQ) [2, 3] defined by

$$\Lambda(\mathbf{M}) = \frac{|\mathbf{p}^H \mathbf{M}^{-1} \mathbf{y}|^2}{(\mathbf{p}^H \mathbf{M}^{-1} \mathbf{p})(\mathbf{y}^H \mathbf{M}^{-1} \mathbf{y})} \underset{H_0}{\overset{H_1}{\gtrless}} \lambda\,, \tag{3}$$

where $\lambda$ is the detection threshold.

However, in most cases, the speckle covariance matrix $\mathbf{M}$ is unknown and this test can not be used in this original form. One solution is to substitute an estimate $\widehat{\mathbf{M}}$ of $\mathbf{M}$ in (2) resulting in an adaptive version of the GLRT:

$$\Lambda(\widehat{\mathbf{M}}) = \frac{|\mathbf{p}^H \widehat{\mathbf{M}}^{-1} \mathbf{y}|^2}{(\mathbf{p}^H \widehat{\mathbf{M}}^{-1} \mathbf{p})(\mathbf{y}^H \widehat{\mathbf{M}}^{-1} \mathbf{y})} \underset{H_0}{\overset{H_1}{\gtrless}} \lambda. \tag{4}$$

It is clear that the estimation accuracy of $\widehat{\mathbf{M}}$ has an important impact on the detection performance. Many applications result in a speckle covariance matrix that exhibits some particular structure. Such a situation is frequently met in radar systems using a symmetrically spaced linear array for spatial domain processing, or symmetrically spaced pulse train for temporal domain processing [4]. In these systems, the clutter covariance matrix $\mathbf{M}$ has the persymmetric property [5]:

$$\mathbf{M} = \mathbf{J}_m\,\mathbf{M}^*\,\mathbf{J}_m\,, \tag{5}$$

where $\mathbf{J}_m$ is the $m$-dimensional antidiagonal matrix having 1 as non-zero elements. The signal vector is also persymmetric, i.e. it satisfies:

$$\mathbf{p} = \mathbf{J}_m \, \mathbf{p}^* \, . \tag{6}$$

The purpose of this paper is to derive an estimate of the speckle covariance matrix based on the secondary data and taking into account its persymmetric structure: it will be called the Persymmetric Fixed-Point estimate ($\widehat{\mathbf{M}}_{PFP}$). The statistical properties of $\widehat{\mathbf{M}}_{PFP}$ are also established and allow to investigate the distribution of the test statistic $\Lambda(\widehat{\mathbf{M}}_{PFP})$. In the last section, results obtained with non-Gaussian real data demonstrate the interest of the proposed detection scheme compared to existing detectors [6].

## II. Problem Statement and Preliminaries

In the context of persymmetric $\mathbf{M}$ and $\mathbf{p}$, the problem defined by (1) will be first reformulated thanks to the following theorem.

**Theorem 1** *Let $\boldsymbol{T}$ be the unitary matrix defined as:*

$$\boldsymbol{T} = \begin{cases} \frac{1}{\sqrt{2}} \begin{pmatrix} \boldsymbol{I}_{m/2} & \boldsymbol{J}_{m/2} \\ i\,\boldsymbol{I}_{m/2} & -i\,\boldsymbol{J}_{m/2} \end{pmatrix} & \textit{for } m \textit{ even} \\ \frac{1}{\sqrt{2}} \begin{pmatrix} \boldsymbol{I}_{(m-1)/2} & \boldsymbol{0} & \boldsymbol{J}_{(m-1)/2} \\ \boldsymbol{0} & \sqrt{2} & \boldsymbol{0} \\ i\,\boldsymbol{I}_{(m-1)/2} & \boldsymbol{0} & -i\,\boldsymbol{J}_{(m-1)/2} \end{pmatrix} & \textit{for } m \textit{ odd.} \end{cases} \tag{7}$$

*Persymmetric vectors and Hermitian matrices are characterized by the following properties:*

- *$\boldsymbol{p} \in \mathbb{C}^m$ is a persymmetric vector if and only if $\boldsymbol{T}\,\boldsymbol{p}$ is a real vector.*
- *$\boldsymbol{M}$ is a persymmetric Hermitian matrix if and only if $\boldsymbol{T}\,\boldsymbol{M}\,\boldsymbol{T}^H$ is a real symmetric matrix.*

*Proof:* The proof is straightforward and involves elementary algebraic manipulations. ■

Using previous theorem, the original problem (1) can be equivalently reformulated as follows. Let us introduce the transformed primary data $\mathbf{z}$, the transformed secondary data $\mathbf{z}_k$, the transformed clutter vector $\mathbf{n}$ and speckle vector $\mathbf{x}$, the transformed signal vector $\mathbf{s}$ defined as:

- for the primary data: $\mathbf{z} = \mathbf{T}\,\mathbf{y}$, $\mathbf{s} = \mathbf{T}\,\mathbf{p}$, $\mathbf{n} = \mathbf{T}\,\mathbf{c}$ and $\mathbf{x} = \mathbf{T}\,\mathbf{g}$;
- for the secondary data: $\mathbf{z}_k = \mathbf{T}\,\mathbf{y}_k$, $\mathbf{n}_k = \mathbf{T}\,\mathbf{c}_k$, $\mathbf{x}_k = \mathbf{T}\;\mathbf{g}_k$.

The transformed speckle covariance matrix is therefore given by $\mathbf{R} = E(\mathbf{x}\,\mathbf{x}^H) = E(\mathbf{x}_k\,\mathbf{x}_k^H) = \mathbf{T}\,\mathbf{M}\,\mathbf{T}^H$.

From Theorem 1, the transformed signal vector $\mathbf{s}$ and the transformed clutter covariance matrix are both real. Then, the original problem (1) is equivalent to:

$$\begin{cases} H_0 : \mathbf{z} = \mathbf{n} & \mathbf{z}_k = \mathbf{n}_k, \text{ for } 1 \le k \le K\,, \\ H_1 : \mathbf{z} = A\,\mathbf{s} + \mathbf{n} & \mathbf{z}_k = \mathbf{n}_k, \text{ for } 1 \le k \le K\,, \end{cases} \tag{8}$$

where $\mathbf{z} \in \mathbb{C}^m$, $\mathbf{n} \sim \mathcal{CN}(\mathbf{0}, \mathbf{R})$, $\mathbf{s}$ is a known real vector, $\mathbf{R}$ is an unknown real symmetric matrix. The $K$ transformed secondary data $\mathbf{z}_k$ are i.i.d and share the same distribution as $\mathbf{n}$. They are given in terms of the texture and the transformed speckle by:

$$\mathbf{n} = \sqrt{\tau}\,\mathbf{x} \text{ and } \mathbf{n}_k = \sqrt{\tau_k}\,\mathbf{x}_k, \tag{9}$$

where $\mathbf{x} \sim \mathcal{CN}(\mathbf{0}, \mathbf{R}), \mathbf{x}_k \sim \mathcal{CN}(\mathbf{0}, \mathbf{R})$. From now on, the problem under study is the problem defined by (8).

The main motivation for introducing the transformed data is that the original persymmetric covariance matrix of the speckle is transformed into a real matrix.

## III. The Persymmetric Fixed-Point Estimate and the Corresponding Adaptive GLRT

### A. The PFP estimate

Conte and Gini in [7], [8] have shown that an approximate maximum likelihood estimate $\widehat{\mathbf{R}}$ of $\mathbf{R}$ is a solution of the following equation:

$$\widehat{\mathbf{R}} = \frac{m}{K} \sum_{k=1}^{K} \left( \frac{\mathbf{n}_k\,\mathbf{n}_k^H}{\mathbf{n}_k^H\,\widehat{\mathbf{R}}^{-1}\,\mathbf{n}_k} \right). \tag{10}$$

Existence and uniqueness of the above equation solution, denoted $\widehat{\mathbf{R}}_{FP}$ have already been investigated in [9]. This equation implies that $\widehat{\mathbf{R}}_{FP}$ is independent of the $\tau_k$'s.

The statistical properties of $\widehat{\mathbf{R}}_{FP}$ have been studied in [10]. Since the transformed speckle covariance matrix $\mathbf{R}$ is real, its structure may be taken into account in the estimation procedure by retaining only the real part of the fixed-point estimate. This leads to the proposed covariance estimate called the Persymmetric Fixed-Point since it results from the persymmetric structure of the original speckle covariance matrix:

$$\widehat{\mathbf{R}}_{PFP} = \mathcal{R}e(\widehat{\mathbf{R}}_{FP}), \tag{11}$$

where $\mathcal{R}e(.)$ denotes the real part of a complex element.

The statistical properties of $\widehat{\mathbf{R}}_{PFP}$ are provided by the following theorem:

**Theorem 2 (Statistical performance of $\widehat{\mathbf{R}}_{PFP}$)**

- *$\widehat{\boldsymbol{R}}_{PFP}$ is a consistent estimate of $\boldsymbol{R}$ when $K$ tends to infinity.*
- *$\widehat{\boldsymbol{R}}_{PFP}$ is an unbiased estimate of $\boldsymbol{R}$.*
- *Its asymptotic distribution is the same as the asymptotic distribution of a real Wishart matrix with $\left(\frac{m}{m+1}\right) 2K$ degrees of freedom.*

*Proof:* Results of Theorem 2 are straightforwardly involved by the statistical analysis of $\widehat{\mathbf{R}}_{FP}$ provided by [7]. ■

This theorem shows that the PFP estimate allows to virtually double the number of secondary data, compared to the original FP estimate.

### B. The adaptive GLRT based on the PFP estimate

The adaptive GLRT for the transformed problem (8) and based on the PFP estimate is:

$$\Lambda(\widehat{\mathbf{R}}_{PFP}) = \frac{|\mathbf{s}^\top \widehat{\mathbf{R}}_{PFP}^{-1} \mathbf{z}|^2}{(\mathbf{s}^\top \widehat{\mathbf{R}}_{PFP}^{-1} \mathbf{s})(\mathbf{z}^H \widehat{\mathbf{R}}_{PFP}^{-1} \mathbf{z})} \underset{H_0}{\overset{H_1}{\gtrless}} \lambda. \quad (12)$$

In this section, the statistical properties of the test statistic $\Lambda(\widehat{\mathbf{R}})$ are investigated under the null hypothesis. Let us recall some basic definitions:

- A test statistic is said to be texture-CFAR (Constant False Alarm Rate) when its distribution is independent of the texture distribution,
- A test statistic is said to be matrix-CFAR when its distribution is independent of $\mathbf{R}$,
- A test statistic is said to be SIRV-CFAR when it is both texture-CFAR and matrix-CFAR.

**Theorem 3** *$\Lambda(\widehat{\mathbf{R}}_{PFP})$ is SIRV-CFAR.*

*Proof:* Since $\widehat{\mathbf{R}}_{PFP}$ does not depend on the texture and since the GLRT-LQ is homogeneous in terms of $\tau$, this leads to the texture-CFAR property of $\Lambda(\widehat{\mathbf{R}}_{PFP})$. Hence, in the sequel, all the statistical analysis (for example PDF derivations) will be considered under Gaussian assumption.

Let us now investigate the matrix-CFAR property. Let $\mathbf{R}^{\frac{1}{2}}\,\mathbf{R}^{\frac{1}{2}}$ be a real factorization of $\mathbf{R}$, and let $\mathbf{Q}$ be a real unitary matrix such that:

$$\mathbf{Q}\,\mathbf{R}^{-\frac{1}{2}}\,\mathbf{s} = \mathbf{e}_1 = (1, 0, 0, \ldots, 0)^\top. \quad (13)$$

Then, the test statistic $\Lambda(\widehat{\mathbf{R}}_{PFP})$ may be rewritten

$$\Lambda = \frac{|\mathbf{e}_1^\top \widehat{\mathbf{W}}^{-1} \mathbf{w}|^2}{(\mathbf{e}_1^\top \widehat{\mathbf{W}}^{-1} \mathbf{e}_1)(\mathbf{w}^H \widehat{\mathbf{W}}^{-1} \mathbf{w})}, \quad (14)$$

where $\mathbf{w} = \mathbf{Q}\,\mathbf{R}^{-\frac{1}{2}}\,\mathbf{c} \sim \mathcal{CN}(0, \mathbf{I})$ and where

$$\begin{aligned} \widehat{\mathbf{W}} &= \mathbf{Q}\,\mathbf{R}^{-\frac{1}{2}}\,\widehat{\mathbf{R}}_{PFP}\,\mathbf{R}^{-\frac{1}{2}}\,\mathbf{Q}^\top \\ &= \mathcal{R}e\left(\mathbf{Q}\,\mathbf{R}^{-\frac{1}{2}}\,\widehat{\mathbf{R}}_{FP}\,\mathbf{R}^{-\frac{1}{2}}\,\mathbf{Q}^\top\right). \end{aligned} \quad (15)$$

It has been shown in [11] that $\mathbf{Q}\,\mathbf{R}^{-\frac{1}{2}}\,\widehat{\mathbf{R}}_{FP}\,\mathbf{R}^{-\frac{1}{2}}\,\mathbf{Q}^\top$ in (15) is a fixed point estimate of the identity matrix and that its distribution is therefore independent of $\mathbf{R}$: thus, the same conclusion holds for its real part $\widehat{\mathbf{W}}$ defined by (15) and the matrix-CFAR property is proved. ■

The analytical expression for the Probability Density Function of the test statistic $\Lambda(\widehat{\mathbf{R}}_{PFP})$ has not been derived but the following theorem gives some insight about its distribution.

**Theorem 4** *For large $K$, $\Lambda(\widehat{\mathbf{R}}_{PFP})$ has the same distribution as $\dfrac{F}{F+1}$ where*

$$F = \frac{(\alpha_1\,u_{22} - \alpha_2\,u_{21})^2 + \left(1 + \left(\dfrac{\beta_3}{u_{33}}\right)^2\right)(a\,u_{22} - b\,u_{21})^2}{(\alpha_2\,u_{11})^2 + \left(t_{11}\,u_{22}\dfrac{\beta_3}{u_{33}}\right)^2 + u_{11}^2\left(1 + \left(\dfrac{\beta_3}{u_{33}}\right)^2\right) b^2} \quad (16)$$

*and where all the following random variables are independent and distributed according to:*

$$\begin{aligned} a, b, \alpha_1, u_{21} &\sim \mathcal{N}(0,1), \\ \alpha_2^2 &\sim \chi^2_{m-1}, \\ \beta_3^2 &\sim \chi^2_{m-2}, \\ u_{11}^2 &\sim \chi^2_{K'-m+1}, \\ u_{22}^2 &\sim \chi^2_{K'-m+2}, \\ u_{33}^2 &\sim \chi^2_{K'-m+3}. \end{aligned} \quad (17)$$

*with $K' = \dfrac{m}{m+1} 2K$.*

*Proof:* Let us start from (14). Then

$$\Lambda(\widehat{\mathbf{R}}_{PFP}) = \frac{|\mathbf{e}_1^\top \widehat{\mathbf{W}}^{-1} (\sqrt{2}\,\mathbf{w})|^2}{(\mathbf{e}_1^\top \widehat{\mathbf{W}}^{-1} \mathbf{e}_1)((\sqrt{2}\,\mathbf{w}^H)\,\widehat{\mathbf{W}}^{-1} (\sqrt{2}\,\mathbf{w}))}, \quad (18)$$

with $\mathbf{w} \sim \mathcal{CN}(\mathbf{0}, \mathbf{I})$ where $(\sqrt{2}\,\mathbf{w}) = \mathbf{w}_1 + i\,\mathbf{w}_2$ with $\mathbf{w}_1$ and $\mathbf{w}_2$ uncorrelated and $\mathcal{N}(\mathbf{0}, \mathbf{I})$ distributed.
Thus

$$\Lambda(\widehat{\mathbf{R}}_{PFP}) = \frac{|\mathbf{e}_1^\top \widehat{\mathbf{W}}^{-1} \mathbf{w}_1|^2 + |\mathbf{e}_1^\top \widehat{\mathbf{W}}^{-1} \mathbf{w}_2|^2}{(\mathbf{e}_1^\top \widehat{\mathbf{W}}^{-1} \mathbf{e}_1)(\mathbf{w}_1^\top \widehat{\mathbf{W}}^{-1} \mathbf{w}_1 + \mathbf{w}_2^\top \widehat{\mathbf{W}}^{-1} \mathbf{w}_2)}.$$

From Theorem 2 and (15), for large $K$, $\widehat{\mathbf{W}}$ is real Wishart distributed with $K' = \dfrac{m}{m+1} 2K$ degrees of freedom. The vectors $\mathbf{w}_1$ and $\mathbf{w}_2$ can be decomposed on an orthonormal vectors triplet $(\mathbf{e}_1, \mathbf{f}_2, \mathbf{f}_3)$:

$$\begin{aligned} \mathbf{w}_1 &= \alpha_1\,\mathbf{e}_1 + \alpha_2\,\mathbf{f}_2 \\ \mathbf{w}_2 &= \beta_1\,\mathbf{e}_1 + \beta_2\,\mathbf{f}_2 + \beta_3\,\mathbf{f}_3. \end{aligned}$$

where $\beta_1$ and $\beta_2$ are independent and $\mathcal{N}(0,1)$ distributed. Moreover $\alpha_1$, $\alpha_2$, $\beta_1$, $\beta_2$, $\beta_3$, $\mathbf{f}_2$ and $\mathbf{f}_3$ are independent.

Let $(\mathbf{e}_1, \mathbf{e}_2, \ldots, \mathbf{e}_m)$ be the canonical basis. Using an appropriate rotation $\mathbf{G}$ such as $\mathbf{G}\,(\mathbf{e}_1, \mathbf{f}_2, \mathbf{f}_3) = (\mathbf{e}_1, \mathbf{e}_2, \mathbf{e}_3)$, $\Lambda(\widehat{\mathbf{R}}_{PFP})$ can be rewritten as

$$\Lambda(\widehat{\mathbf{R}}_{PFP}) = \frac{|\mathbf{e}_1^\top \widehat{\mathbf{Z}}^{-1} \mathbf{v}_1|^2 + |\mathbf{e}_1^\top \widehat{\mathbf{Z}}^{-1} \mathbf{v}_2|^2}{(\mathbf{e}_1^\top \widehat{\mathbf{Z}}^{-1} \mathbf{e}_1)(\mathbf{v}_1^\top \widehat{\mathbf{Z}}^{-1} \mathbf{v}_1 + \mathbf{v}_2^\top \widehat{\mathbf{Z}}^{-1} \mathbf{v}_2)},$$

where $\mathbf{v}_1 = \mathbf{G}\,\mathbf{w}_1$, $\mathbf{v}_2 = \mathbf{G}\,\mathbf{w}_2$ and $\mathbf{G}\,\widehat{\mathbf{W}}^{-1}\,\mathbf{G}^{-1} = \widehat{\mathbf{Z}}^{-1}$.

Using Bartlett's decomposition $\mathbf{Z} = \mathbf{U}^\top\mathbf{U}$ for Wishart matrices [12] where $\mathbf{U} = (u_{i,j})_{1 \leq i \leq j \leq m}$ is an upper triangular matrix whose random elements are independent and distributed as:

$$u_{i,i}^2 \sim \chi^2_{K'+i-m} \text{ and } u_{i,j} \sim \mathcal{N}(0,1) \text{ for } i < j.$$

Moreover let $u'_{i,j}$ be the elements of the matrix $\mathbf{U}^{-1}$. We define:

$$\begin{aligned}\alpha &= \frac{|\mathbf{e}_1^\top \widehat{\mathbf{Z}}^{-1} \mathbf{v}_1|^2 + |\mathbf{e}_1^\top \widehat{\mathbf{Z}}^{-1} \mathbf{v}_2|^2}{(\mathbf{e}_1^\top \widehat{\mathbf{Z}}^{-1} \mathbf{e}_1)}, \\ &= (\alpha_1 \, u'_{11} + \alpha_2 \, u'_{21})^2 + (\beta_1 \, u'_{11} + \beta_2 \, u'_{21} + \beta_3 \, u'_{31})^2,\end{aligned}$$

and

$$\begin{aligned}\beta &= \mathbf{v}_1^\top \widehat{\mathbf{Z}}^{-1} \mathbf{v}_1 + \mathbf{v}_2^\top \widehat{\mathbf{Z}}^{-1} \mathbf{v}_2, \\ &= \alpha + (u'_{22} \, \alpha_2)^2 + (u'_{22} \, \beta_2 + u'_{32} \, \beta_3)^2 + (u'_{33} \, \beta_3)^2.\end{aligned}$$

We deduce that $\Lambda = \dfrac{\alpha}{\alpha+\beta} = \dfrac{\alpha/\beta}{1+\alpha/\beta} = \dfrac{F}{1+F}$ with

$$F = \frac{(\alpha_1 \, u'_{11} + \alpha_2 \, u'_{21})^2 + (\beta_1 \, u'_{11} + \beta_2 \, u'_{21} + \beta_3 \, u'_{31})^2}{(u'_{22} \, \alpha_2)^2 + (u'_{22} \, \beta_2 + u'_{32} \, \beta_3)^2 + (u'_{33} \, \beta_3)^2}.$$

Bartlett's decomposition gives the elements of $\mathbf{U}^{-1}$:

$$\begin{aligned}u'_{11} &= \frac{1}{u_{11}}, \\ u'_{22} &= \frac{1}{u_{22}}, \\ u'_{21} &= -\frac{u_{21}}{u_{11} \, u_{22}}, \\ u'_{33} &= \frac{1}{u_{33}}, \\ u'_{32} &= -\frac{u_{32}}{u_{22} \, u_{33}}, \\ u'_{31} &= -\frac{1}{u_{11}} \left( \frac{u_{31}}{u_{33}} - \frac{u_{32} \, u_{21}}{u_{22} \, u_{33}} \right). \qquad (19)\end{aligned}$$

After some basic manipulations, $F$ can be expressed as (16) which concludes the proof. ■

Theorem 4 may be used to obtain, through Montecarlo simulations, the relation between the Probability of False Alarm and the threshold $\lambda$ for the GRLT-PFP (12).

## IV. Application on Experimental Data

Based on experimental data, this section shows the improvement in detection performance of the adaptive GLRT based on the PFP estimate compared to the GLRT based on the FP estimate. The ground clutter data used in this paper were collected by an operational radar at Thales Air System. The radar was 13 meters above ground and illuminating the ground at low grazing angle. Ground clutter complex echoes were collected in $N = 868$ range bins for 70 different azimuth angles and for $m = 8$ pulses, which means that vectors size is $m = 8$. Figure 1 displays the Ground clutter data level (in dB) corresponding to the first pulse echo. Near the radar, echoes characterize non-Gaussian heterogeneous ground clutter whereas beyond the radioelectric horizon of the radar (around 15 kms) only Gaussian thermal noise (the blue part of the map) is present.

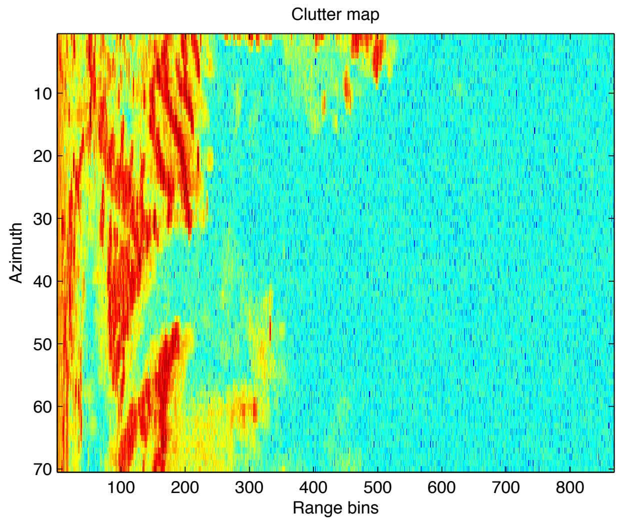


Fig. 1. Ground clutter data level (in dB) corresponding to the first pulse.

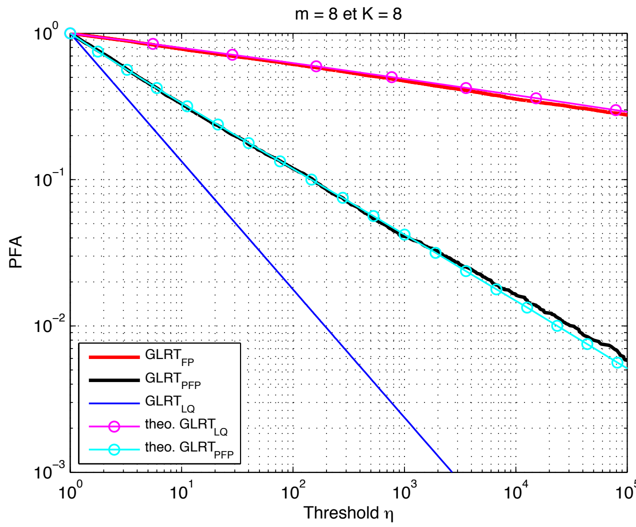


Fig. 2. Probability of false alarm for the three detectors with $\eta = \frac{1}{(1-\lambda)^m}$ ($3 \times 3$ mask).

Figures 2 and 3 give the Probability of False Alarm ($PFA$) as a function of the threshold, for different numbers $K$ of secondary data, for the following three detectors : GLRT-LQ, GLRT-FP and GLRT-PFP. The GLRT-LQ is just used as a benchmark for comparison: it can not be used in practice since it assumes that the speckle covariance matrix is known. The GLRT-FP and the GLRT-PFP use as secondary data the $K$ cells surrounding the cell under test. The experimental detection threshold is determined by counting, moving the CFAR-mask. Moreover, theoretical results based on the

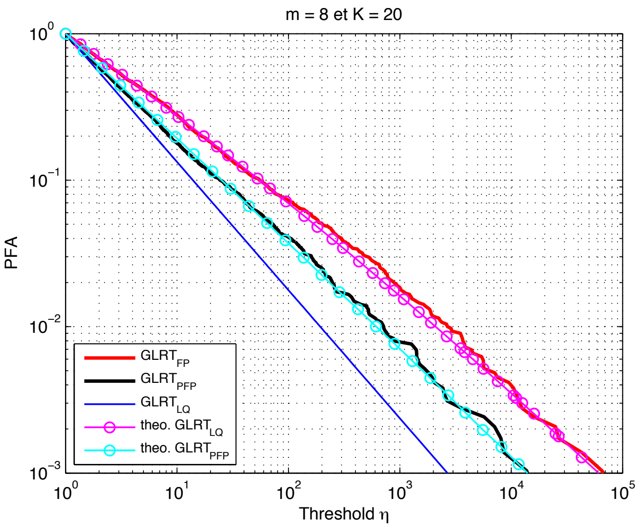


Fig. 3. Probability of false alarm for the three detectors with $\eta = \frac{1}{(1-\lambda)^m}$ ($7 \times 3$ mask).

asymptotic Wishart distributions of $\widehat{\mathbf{R}}_{FP}$ and $\widehat{\mathbf{R}}_{PFP}$ (circle lines) are displayed: it can be noticed that experimental results are in very good agreement with the theory.

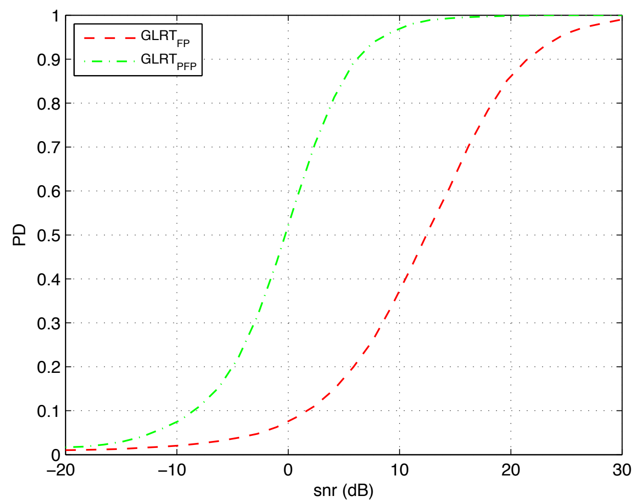


Fig. 4. Probability of detection for the GLRT-FP and GLRT-PFP ($PFA = 10^{-2}, m = 8, K = 8$).

Figures 4, 5 and 6 show the experimental Probability of Detection ($PD$) as a function of the Signal to Noise Ratio, for different numbers $K$ of secondary data, with $PFA = 10^{-2}$ for the GLRT-FP and the GLRT-PFP. The first figure shows a spectacular 12 dB improvement in detection performance of the GLRT-PFP over the GLRT-FP for $P_d = 0.5$. Indeed, to inverse the covariance matrix estimate, one needs to assume that $K \geq m$ while for the PFP, this number is virtually doubled. The second figure corresponds to the classical

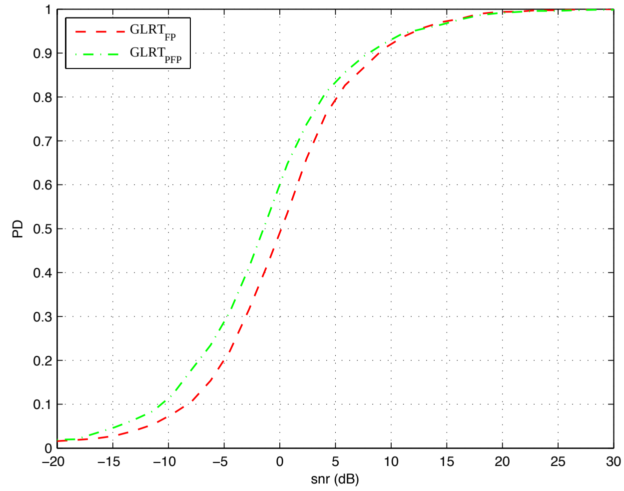


Fig. 5. Probability of detection for the GLRT-FP and GLRT-PFP ($PFA = 10^{-2}, m = 8, K = 16$).

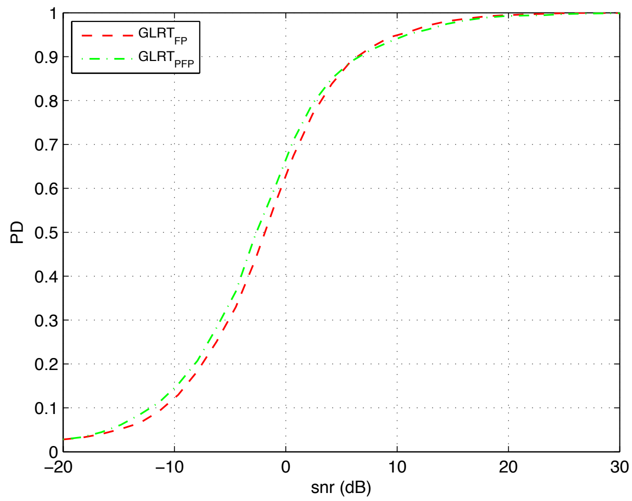


Fig. 6. Probability of detection for the GLRT-FP and GLRT-PFP ($PFA = 10^{-2}, m = 8, K = 20$).

choice $K = 2m$ which is the admitted limiting value for acceptable performance degradation less than 3 dB. The last figure shows a less clear improvement due to the higher number of secondary data.

These results clearly demonstrate the interest of taking into account the persymmetric structure of the speckle covariance matrix in adaptive detection, especially for $m \leq K \leq 2m$. Indeed, classical adaptive detection schemes are well known to yield poorer performance when $K \leq 2m$.

## V. Conclusion

In this paper, an extended version of the Generalized Likelihood Ratio Test - Linear Quadratic (GLRT-LQ ) has been derived by exploiting the persymmetric structure of the covariance matrix in the case of non-Gaussian clutter modeled by Spherically Invariant Random Vectors. The persymmetry assumption allows to transpose the classical problem into a real context (especially for the covariance matrix and the steering vector) and leads to an improved covariance matrix estimation, called the Persymmetric Fixed Point (PFP). The statistical analysis of this estimate has been derived: the PFP estimate exhibits good performance. Replacing it in the GLRT-LQ provides a new adaptive detector, called the GLRT-PFP, whose detection performance are widely improved in comparison to the GLRT-FP. This is explained by the fact that the PFP estimate is virtually built with twice more data than the GLRT-FP. These results have been validated by experimentations on real data.

## VI. Acknowledgement

Authors would like to thank Thales Air System for the analysis of their experimental data.

## References


[1] J.B. Billingsley, "Ground Clutter Measurement for Surface Sited Radar," *MIT Technical report 780*, February 1993.

[2] E. Conte, M. Lops, and G. Ricci, "Asymptotically Optimum Radar Detection in Compound-Gaussian Clutter," *IEEE Trans. on Aerosp. Electron. System*, vol. 31, pp. 617–625, April 1995.

[3] F. Gini, "Sub-Optimum Coherent Radar Detection in a Mixture of K-Distributed and Gaussian Clutter," *IEE Proc. on Radar, Sonar Navig.*, vol. 144, pp. 39–48, February 1997.

[4] L. Cai and H. Wang, "A Persymmetric Multiband GLR Algorithm," *IEEE trans. on Aerosp. Electron. System*, pp. 806–816, July 1992.

[5] E. Conte and A. De Maio, "Exploiting Persymmetry for CFAR Detection in Compound-Gaussian Clutter," *IEEE trans. on Aerosp. Electron. System*, vol. 39, pp. 719–724, April 2003.

[6] M. Casillo, A. De Maio, S; Iomelli, and L. Landi, "A Persymmetric GLRT for Adaptive Detection in Partially-Homogeneous Environment," *IEEE Signal Processing Letters*, vol. 17, pp. 1016–1019, December 2007.

[7] F. Gini and M. V Greco, "Covariance matrix estimation for CFAR detection in correlated heavy tailed clutter," *Signal Processing, special section on Signal Processing with Heavy Tailed Distributions*,, vol. 82, pp. 1847–1859, December 2002.

[8] E. Conte, A. De Maio, and G. Ricci, "Recursive estimation of the covariance matrix of a compound-Gaussian process and its application to adaptive CFAR detection," *IEEE Trans. on Sig. Proc.*, vol. 50, pp. 1908ñ1915, August 2002.

[9] F. Pascal, Y. Chitour, J.P. Ovarlez, P. Forster, and P. Larzabal, "Covariance Structure Maximum Likelihood Estimates in Compound Gaussian Noise: Existence and Algorithm Analysis," *IEEE Trans. on Sig. Proc., accepted for future publication*, 2007.

[10] F. Pascal, P. Forster, J.P. Ovarlez, and P. Larzabal, "Performance Analysis of Covariance Matrix Estimate in Impulsive Noise," *IEEE Trans. on Sig. Proc., accepted for publication*, 2007.

[11] F. Pascal, J.P. Ovarlez, P. Forster, and P. Larzabal, "On a SIRV-CFAR Detector with Radar Experimentations in Impulsive Noise," *Proc. EUSIPCO*, September 2006.

[12] R.J. Muirhead, "Aspects of Multivariate Statistical Theory," *Wiley, New-York*, 1982.